Dynamic simulations of multiphase flow in bubble columns

G. M. Cartland Glover, [a*] S. C. Generalis [a*] and N. H. Thomas [a, b]

[a] Aston University, School of Engineering and Applied Science, Division of Chemical Engineering and Applied Chemistry, Birmingham, B4 7ET U. K. (Tel +44 (0)121 359 3611) cartlgm1@aston.ac.uk*, S.C.Generalis@aston.ac.uk,

[b] FRED Ltd, Aston Science Park, Birmingham B7 4JB U. K. Nhtfred@aol.com.
* corresponding authors

Keywords: bubble column, computational fluid dynamics, CFD, gas-liquid-solid flow, bioreactors, food industry

Abstract
The aim of this paper is to introduce tracker particles to capture the hydrodynamics of support beads used in gas-liquid-solid biological reactors through the use of computational fluid dynamics. The gas-liquid interactions were modelled using an algebraic slip mixture model, where the gas and liquid phases are treated as a pseudo-continuous mixture. The interactions between the gas and liquid phases are calculated as force terms in the momentum conservation equation. With this model and the standard k-ε turbulence model, the turbulent motion of gas-liquid flow is captured for a representative case of bubble column with an aspect ratio of 5:1.[1, 2, 3] A superficial gas velocity of 0.02 m s^{-1} returned vertical velocities of 0.15 ± 0.02 m s^{-1} at a height of 2.5 column diameters, this is a reasonable value for a column of less than 0.2 m diameter. In the two-dimensional case the two large eddies developed, showing the overall flow structure, though the flow was stable. For the three-dimensional case a dominant mode with a frequency of 4 min^{-1}, which took 20 seconds to develop after the initialisation of the flow field. Particles were injected into the flow regime and generally followed the motion of the vortical structures present, this was due to the low density of the particles with respect to the liquid phase, leading to lows levels of particle slip. The motion of the particles was analysed by assessing the direction in which the particles were travelling within the column, leading to a measure of the mixing properties in different parts of the column.

1.0 INTRODUCTION

In the food industry, products such as citric acid, ethanol and beer are produced in biological reactors. For some micro-organisms, the most practicable method is to use support beads on which these organisms grow. How these beads move through the liquid phase is important to the growth of the organisms, as the particles will move through regions of varying concentrations of the substrates. Changes in the concentration of dissolved oxygen and other substrates will have an important effect on the metabolic processes that take place and therefore effect the growth and production rates for the organisms. And from this the aims are to study the movement of solid particles and to determine whether the computational fluid dynamic (CFD) models used are adequate for further assessment of the transport and reaction processes occurring in biological reactors. The use of CFD to model multiphase flow in bubble columns has advance gradually over the past decade. With Svendsen and Torvik[4] initially modelled the flow of air bubbles through a column of liquid with no net flow of

liquid in or out of the column, though the flow was modelled using steady state formulations for two-dimensions. Ranade [5,6] investigated the effect of the bubble wake models on the overall structure of bubble column flow in both two and three dimensions for steady flows. Sokolichin, Eigenberger, Lapin and Lüebbert[7, 8, 9, 10, 11, 12, 13] have been prolific in the discussion of the effects that influence the numerical solution of two-fluid and discrete particle models.[12] Of the two models studied, the two-fluid or Euler/Euler model was presented as efficient, but globally based model which portrays the gas phase as a inter-penetrating pseudo-continuous phase in a continuous liquid phase. Whereas the discrete particle model or Langrange/Euler model captures the localised interactions of the gas phase as particles in a continuous liquid phase. Their work has influenced the simulation of bubble columns through the application of modelling techniques by including in their discussions' the effects of discretisation procedures,[12, 13] mesh formation,[8, 12, 13] mathematical phase definition and the comparison of steady and unsteady flow models.[12] Delnoij et al.[14, 15, 16, 17] developed a discrete particle model for two[14] and three-dimensional flows,[17] and discussed the effect of column height to diameter ratios on the flow regimes present. Visual comparisons with experimental investigations[18] were made from the change in the flow phenomena with the change in aspect ratio, with the cooling tower effect observed for a 1:1 column and two distinct flow regions for columns with a height greater than 7:1[16]. This work has required detailed correlation with relevant experimental data to prove that the simulations match reality. This has been difficult to achieve due to problems associated with providing enough data to compare results. With difficulties in obtaining the large quantities of experimental data required in comparing instantaneous or time-averaged profiles of variables such as the vertical velocity or gas phase hold up which can be used to characterise the turbulent flow regimes.

In §2 the models used to track the movement of the particles through the liquid phase, and the boundary conditions applied to the models are described. The results are discussed in section §3, with the conclusions in §4 and the model equations listed in §5.

2.0 INVESTIGATIONS

2.1 Fluid Dynamic Models

The Algebraic Slip Mixture (ASM) model was adapted by Manninen et al.[19] to create a multi-dimensional model which was incorporated into the Fluent computational fluid dynamics software.[1, 20] This model describes the flow regime as an incompressible single-phase pseudo-continuous mixture of the gaseous and liquid phases. The solution scheme used is based upon the closure procedures presented by Ishii,[21,22] Drew,[23,24] Gidaspow,[25] Simonin,[26] Ungarish[27] and Verloop.[28] In this model a single momentum equation is modified to depict the gas and liquid phase as an inter-penetrating mixture phase, calculating the interphase interaction as an extra force term using drift or slip velocity formulations. Continuity and volume fraction equations for each phase are used to ensure conservation laws are maintained and to infer the velocity for each phase.[19] The main reason for using this model is due the increased run-time efficiency when compared with the two-fluid or discrete particle models. There is a limitation to the reliability of this model and it is based around the viscosity formulation used to calculate the mixture phase viscosity, due flaws relating to the volumetric partitioning of the domain used. A more reliable solution can be obtained if empirical formulations are used to calculate the viscosity.

The ASM model was used in conjunction with the k-ε turbulence model[29] in an attempt to include the effects of generation and dissipation of turbulent energy. The main reason for using turbulence models is that the mesh used is to coarse to include all scales of the turbulent

vortices produced by the bubbling of the gas phase in a liquid column. The k-ε turbulence model[29] has been used by Krishna et al.[2] Pfleger[30] et al. Sanyal et al.[1] Sokolichin and Eigenberger[12, 13] to some degree of success. In the turbulence equations in §5 there is a term for the generation of turbulent energy due to buoyancy effects, this term may not have much of an effect on the overall hydrodynamics of the flow regime. Though the inclusion of this term may add further to the complexity of solution procedure and not give a significant improvement in the results obtained. A discrete phase model[20] (DPM) is used to describe the movement of solid particles in a fully developed flow field. The equations used in the predictive models can be found in §5.

2.2 Test Cases

To compare the CFD model results with experimental results two cases were run using the Fluent software on a Pentium II 450 MHz processor (OS = Windows NT). The case describes the flow phenomena for air-water bubbling beds (air density = 1.225 kg m^{-3}; water density = 998.2 kg m^{-3}; air viscosity = 1.7894 * 10^{-5} kg m^{-1} s^{-1}; water viscosity = 1.003 * 10^{-3} kg m^{-1} s^{-1}). The 5:1 column used in experiments,[2] consisted of a distributor plate with 156, 0.5 mm diameter inlets partially aerating the column. The diameter of the column was 0.19 m with a liquid height of the column was 1.045 m and the orifice pitch was 1.25 cm to the centreline of each orifice, from which gas with a superficial gas velocity of 0.02 m s^{-1} was injected.[2] To provide a comparison between the experimental and CFD cases, part of the base of the column grid was defined as an inlet. The boundary conditions applied to the column grid include a bubble diameter of 5 mm and a superficial gas velocity of 0.02 m s^{-1} for an air-water bubble column. These conditions were used for both the three-dimensional and two-dimensional cases. Figure 1 shows the grid used for the two-dimensional case (38 by 104 mesh cells; case A), with the three-dimensional (19 across by 20 around the circumference by 70 mesh cells high; case B) case having a similar form.

The solver specifications for the discretization of the domain involved the following procedures body force weighted for pressure, QUICK[31] for momentum, SIMPLEC[32] for the velocity-pressure coupling and a first-order discretization scheme for the volume fraction and unsteady state, laminar flow models. The under-relaxation factors, which determine how much control each of the equations has in the final solution, were set to 0.3 for the pressure, 0.7 for the momentum, 0.2 for slip velocity equations. The under relaxation factors for the density, body forces and volume fraction were set to 1. The k-ε turbulence model was also applied to the flow model to provide a basic tool to model the complicated phenomena and the transition to turbulence associated with gas-liquid flow in bubble columns. The under-relaxation factors for the transport equations used in the model were set to 0.8.

Four further cases were considered in the DPM simulation for the investigation into the motion of 100 particles in the flow domain, after 200 seconds of simulation time. The diameter of the particles was defined as 5 mm, with densities of 1000 and 1100 kg m^{-3} for both cases A and B. The particles were initially positioned 2 cm apart in the horizontal and 10 cm apart in the vertical directions, in a flat plane across the column.

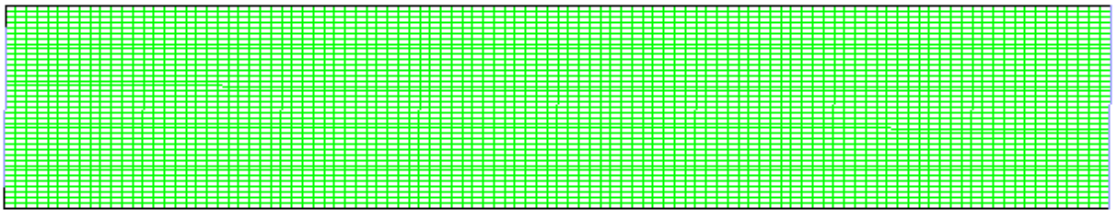

Figure 1: Diagram of the two-dimensional mesh used, where the vertical direction is from left to right.

3.0 RESULTS AND DISCUSSION

The 5:1 bubble column modelled by Sanyal et al.[1] showed the capabilities of the Fluent code in modelling multiphase flow in bubble columns. Using similar boundary conditions the vector fields in Figure 2 and the velocity profiles in Figure 3 were produced for the two and three-dimensional meshes. In Figure 2 the velocity field between the two cases varies from being symmetric in two dimensions, to being asymmetric in three. The velocities range from approximately |0.2| m s^{-1} (magnitude of the largest vectors) to 10^{-20} m s^{-1} (magnitude of the smallest vectors). The three-dimensional plots reveal a similar nature to the vector plots of experimental data.[2] The velocity profiles in Figure 3 can be compared with reasonable accuracy to the experimental profile.[2] The point at which the profiles in Figure 3 cross the abscissa for case B is within 10% of the experimental case, but the difference between case A and the experimental data is greater than 10% for this point. The small difference between in the average velocity profile between cases A and B suggests that two dimensional studies will only provide a partial solution relating to the complicated structure which are present in three dimensions. Figure 4 shows the variation in the vertical velocity at a height of 0.53 m for both case A and B. The flow regime takes 10 to 15 seconds to become fully developed into an oscillating pattern. The case A data shows a similar profile, although the change in velocity is much smaller than for case B. In particular the conjecture here is that strong oscillatory behaviours between the two states of figures 2b and 2c is possibly due to a "connection" or "bridge" between non-linear steady state solutions that enables the transition from one state to another. Such a state does not exist in two dimensions, which in turn means there is no oscillatory behaviour observed. The reasons for the smooth curves can be attributed to the time step size of 0.2 seconds. This time step size will ignore much of the smaller scale oscillations in the flow regime, which occur in turbulent flow situations.

The movement of particles tends to follow the large-scale circulation patterns, with much of the flow in the centre of the column moving upwards, with downward movement near the column walls. As Figure 5 shows the particles near the wall will move down the column and then across into the centre of the column, when the particle reaches bottom of the vortex in which it is travelling. The trajectory completes its full cycle because when at the centre of the column the particle moves back up the column. The variation in the trajectory of the particles in Figure 5 on the density of the particle, as buoyancy has an influence on the nature of bubble column flow. Particles with a density equal to the density of the medium show a greater intensity of movement than the heavier particles in the upward direction. Figures 6 and 7 are charts showing how much the particles move up and down the column. This was achieved by assessing the direction in which a particle crossed a horizontal slice of the column. Each number on the horizontal axis of the chart represents the height of the slice where the assessment of the particle motion was made. For case A the particles of with a density equal to that of the liquid phase, showed the most movement. With more than 200 occurrences of upwards and downwards movement through the horizontal cross sections between 20 and 90

cm of column height and the least activity occurring in the upper and lower cross sections of the column. The other cases show reduced movement, this is due to the stagnation of particles at the top of the column, due to the definition of the liquid surface boundary condition as a free-slip wall or outlet, which prevents the movement towards the column walls. Also the gravitational influence of the heavier particles may limit the upward movement, as these particle will have a settling velocity interaction which will negate the effect of the upward motion of the liquid phase to some extent.

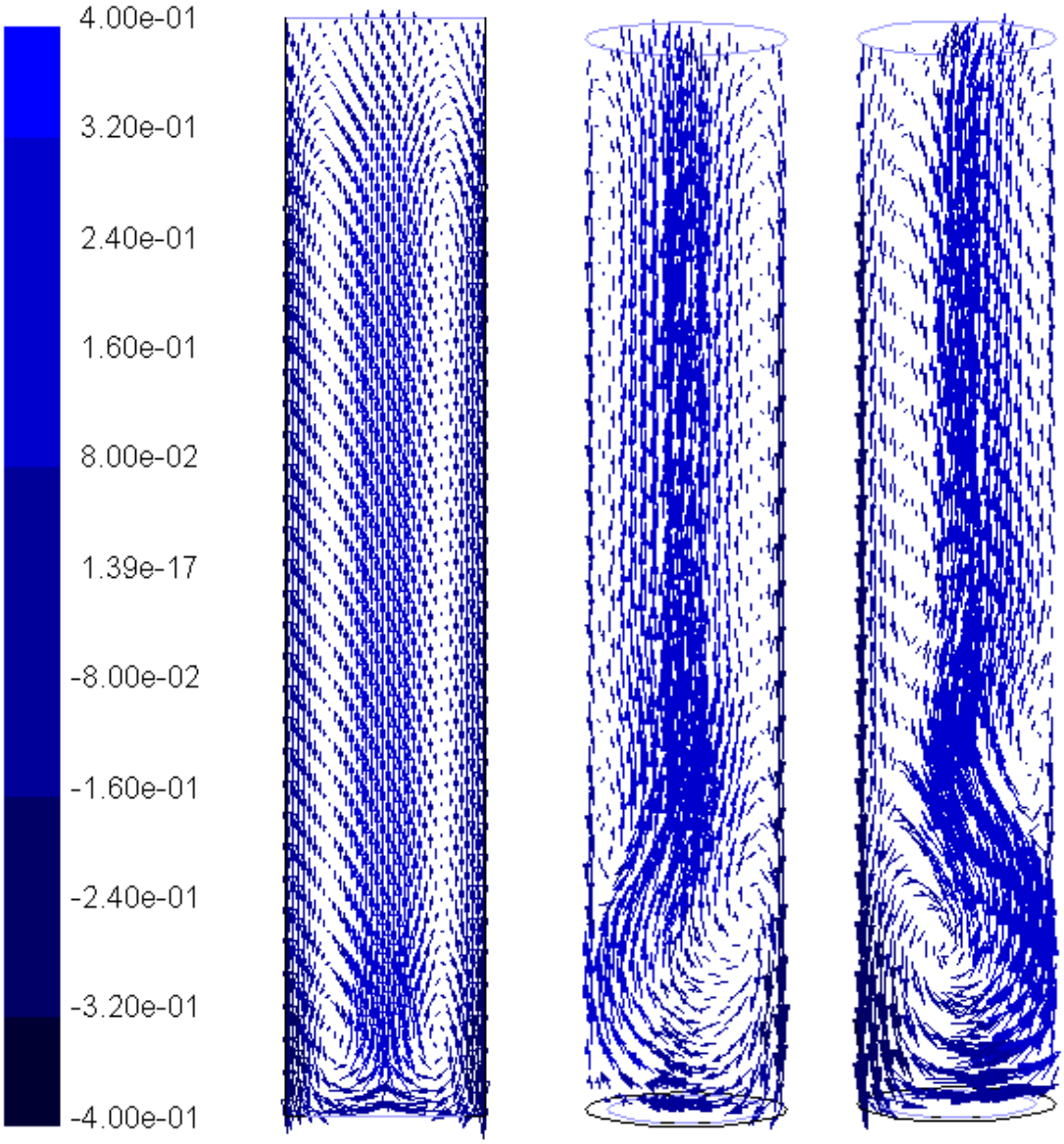

Figure 2: Vector fields for a bubble column an aspect ratio of 5:1, with a superficial gas velocity of 0.02 m s^{-1}: a) 2D case. b) (y-z) cross section of the 3D case. c) (y-x) cross section of the 3D case.

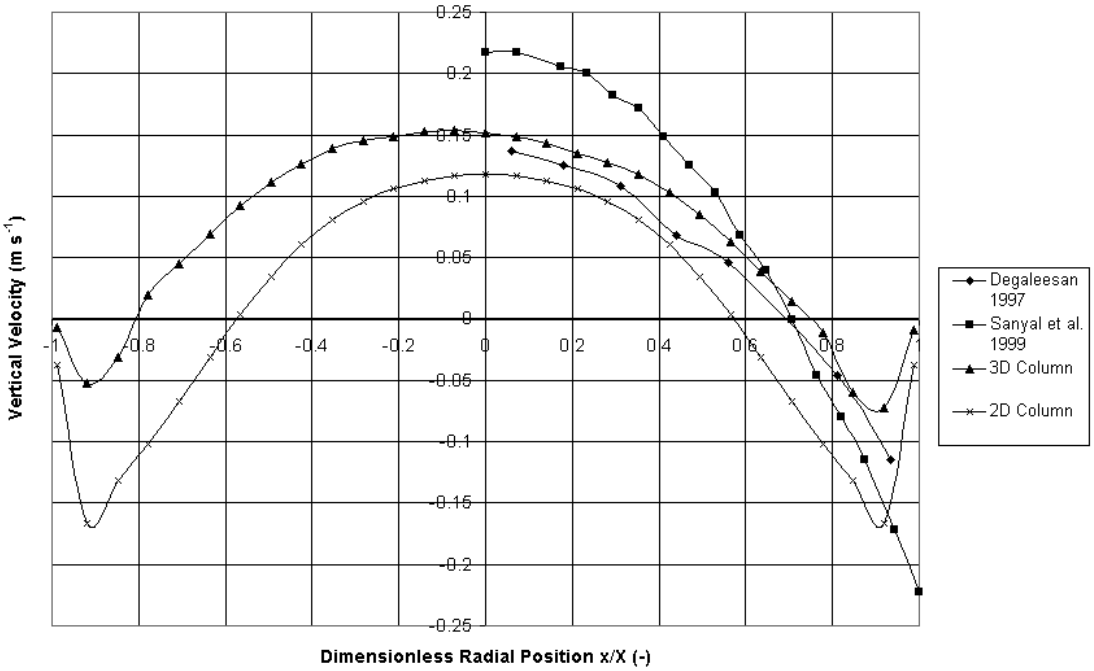

Figure 3: The time averaged velocity profiles for a 5:1 column, at a height of 0.53 m above the base of the column.[1,2]

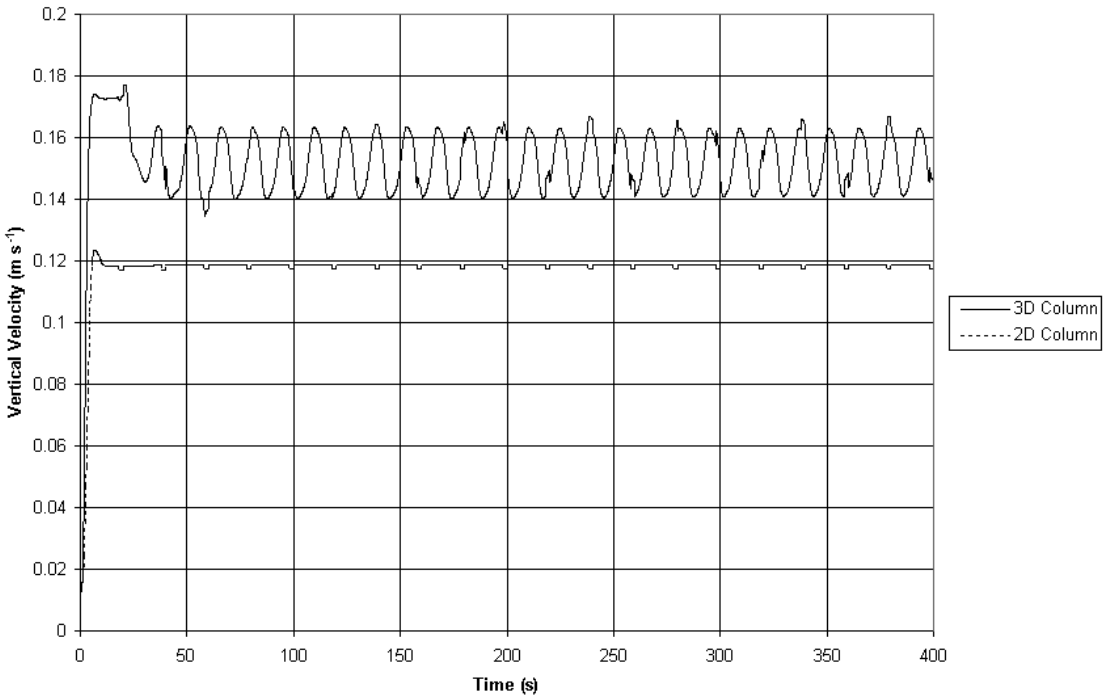

Figure 4: Vertical velocity on the column centre line at a height of 0.53 m.

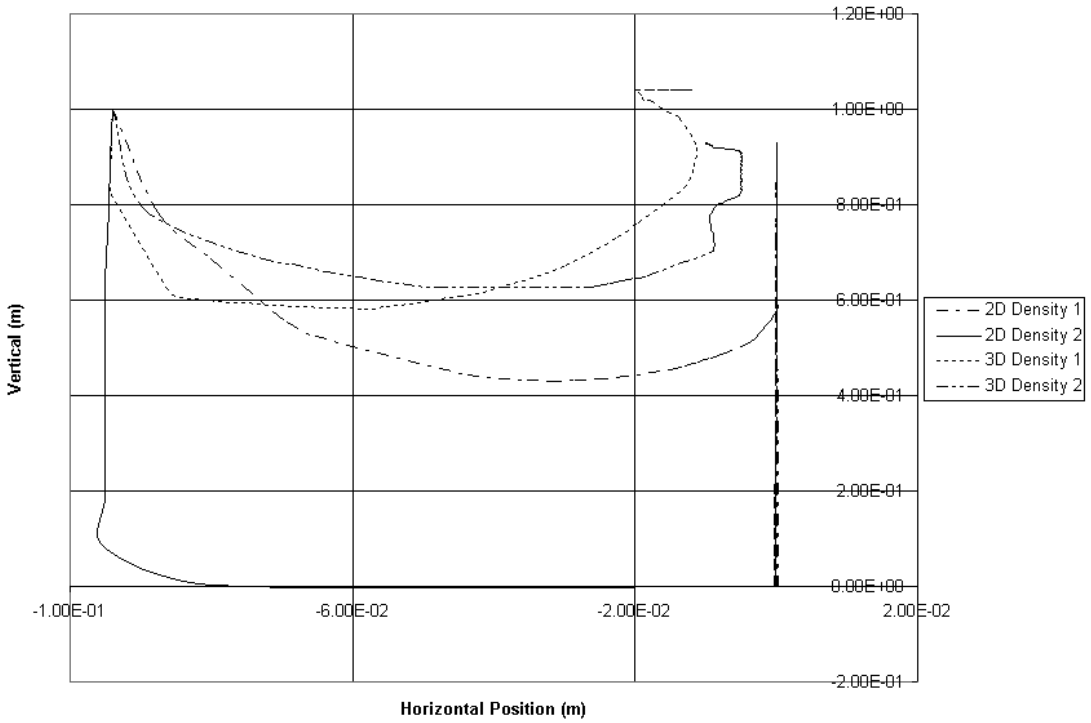

Figure 5: Particle tracks for 20 seconds of flow simulations, where each particle has a different density (Density 1 = 1000 kg m^{-3}; Density 2 =1100 kg m^{-3}). The particles are injected at a location -0.094 m from the centre line by 1 m from the base of the column.

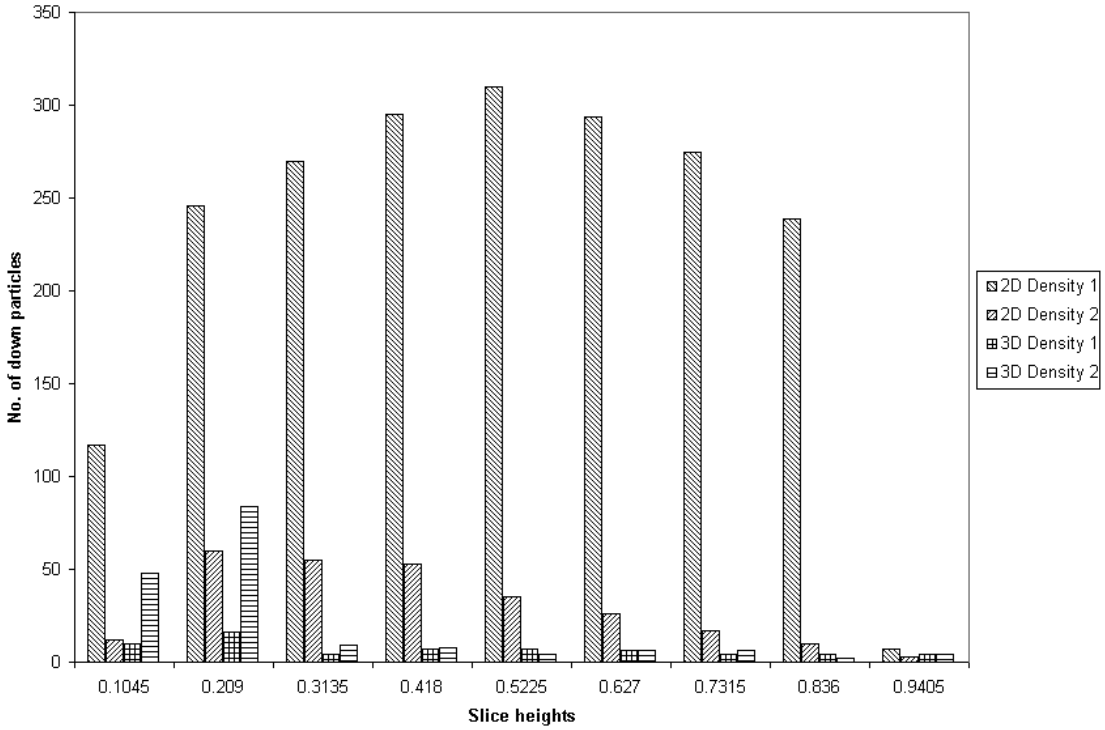

Figure 6: Chart of the number of particles crossing through slices of the column while the particles are moving down the column.

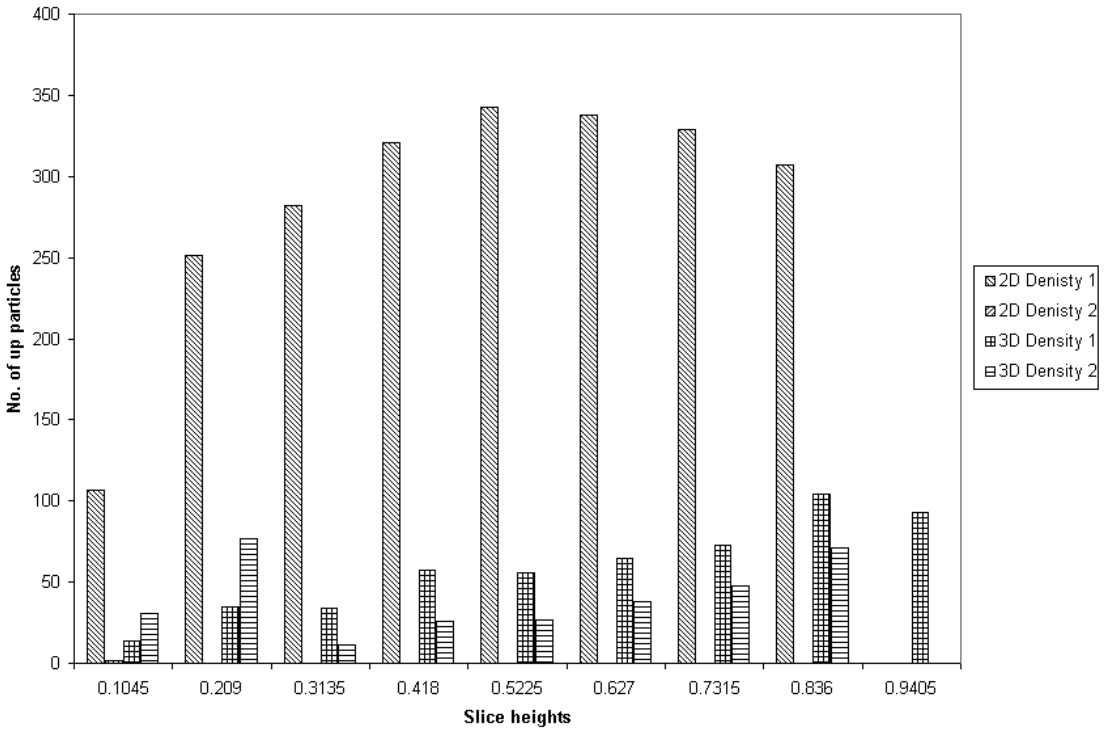

Figure 7: Chart of the number of particles passing through slices of the column while the particles are moving up the column.

4.0 CONCLUSIONS

The simulation of bubble column flow with an algebraic slip mixture model used in conjunction with the standard k-ε turbulence model showed reasonable agreement between the time averaging of vertical velocity profiles obtained from simulations and laboratory work was observed.[1, 2] Case A, the two-dimensional case presented a symmetrical flow field with little or no changes in state were observed. Case B, the three-dimensional case provided simulated data, which showed changes in state, through the change in flow structure in Figure 2 and the change in velocity in Figure 4. Convergence of both cases (2D and 3D) was in the order of $1*10^{-3}$ for residuals of the continuity equation and $1*10^{-5}$ for the momentum and turbulent flow parameters.

The study of the motion of a solid particle phase was studied. Particles with a density equal to that of the liquid phase and particles with a slightly higher density were injected into the fully developed flow regime of a bubble column. The particles followed the overall vortical structures present. A method was used to establish general motion of the particles in the vertical direction, by assessing which direction the particles moved through horizontal cross sections of the domains used. More movement was observed with the lower density particles, than with the heavier particles. The general trend for the motion of the particles after 20 seconds of simulation was to move up the centre and down at the walls. Longer simulation times for the motion of the particles would give an improved idea of the time taken for particle to circulate from the top to the bottom of the column. The problems of increased accuracy of the results of the simulations may be addressed by the increasing the meshes used in this study or the adjustment of k-ε turbulence parameters.

Acknowledgements
We would like to acknowledge Mr M. Overd, for his assistance in analysing the particle data, Fluent Europe Ltd and the support of Inco-Copernicus Grant number ERB IC15-CT98-0904 for enabling this work to be presented, and we would like to dedicate this paper to the memory of Dr. J. Zahradnik.

Appendix: Mathematical Model Equations

These are:

1. The continuity equation for the mixture phase,

$$\frac{\partial}{\partial t}\left(\rho_m\right)+\frac{\partial}{\partial x_i}\left(\rho_m u_{m,i}\right)=0$$

2. The momentum equation for the mixture, where on the right hand side the forces acting on the mixture phase are collected together and include the effects of pressure, viscous stress, gravitational forces, momentum sources and interphase momentum interactions,

$$\frac{\partial}{\partial t}\left(\rho u_{m,j}\right)+\frac{\partial}{\partial x_i}\left(\rho_m u_{m.i} u_{m.j}\right)=$$

$$-\frac{\partial p}{\partial x_j}+\frac{\partial}{\partial x_j}\mu_m\left(\frac{\partial}{\partial x_j}\left(u_{m,i}\right)+\frac{\partial}{\partial x_i}\left(u_{m,j}\right)\right)+\rho_m g_j+F_j+\frac{\partial}{\partial x_i}\sum_{k=1}^{n}\alpha_k\rho_k u_{Dk,i}u_{Dk,j}$$

3. The volume fraction equation, which is used to evaluate the interphase volume fraction variations between the dispersed and continuous phases,

$$\frac{\partial}{\partial t}\left(\alpha_p\rho_p\right)+\frac{\partial}{\partial x_i}\left(\alpha_p\rho_p u_{m,i}\right)=-\frac{\partial}{\partial x_i}\left(\alpha_p\rho_p u_{Dp,i}\right)$$

4. Mixture Density,

$$\rho_m=\sum_{k=1}^{n}\alpha_k\rho_k$$

5. Mixture Viscosity,

$$\mu_m=\sum_{k=1}^{n}\alpha_k\mu_k$$

6. Mass Averaged Velocity,

$$\vec{u}_m=\frac{\sum_{k=1}^{n}\alpha_k\rho_k\vec{u}_k}{\rho_m}$$

7. The drift and slip velocity equations which are used to assess the interphase interactions between the gas and liquid phases:

$$\vec{u}_{D,k} = \vec{u}_k - \vec{u}_m = \vec{V}_{k,c} - \frac{1}{\rho_m}\sum_{i=1}^{n-1}\alpha_k \rho_k \vec{v}_{i,c}$$

$$\vec{V}_{qp} = \vec{u}_p - \vec{u}_q$$

$$\vec{V}_{k,c} = \frac{(\rho_m - \rho_k)}{18\mu_c f}\left(g_j - \frac{D\vec{u}_m}{Dt}\right)$$

8. Friction factor is used to assess the drag forces acting on the dispersed phase, as the gas bubbles move through the liquid phase, typical values of Reynolds number for the simulation are to the order of 10^4.

f = 0.018Re Re>1000

9. The turbulent transport model used to represent the effects of energy generation and dissipation was the k-ε turbulence model[17]. The first transport equation models the turbulent kinetic energy and the second equation models the rate of dissipation of energy from the turbulent flow. G_k and G_b represent the generation of turbulent kinetic energy with respect to the mean velocity gradient and the influence of buoyancy. σ_k and σ_ε are the turbulent Prandtl numbers for the kinetic energy and the rate of dissipation of energy, where $C_{1\text{-}3\varepsilon}$ and C_μ are constants. The third equation refers to the turbulent vicosity estimation.

$$\rho\frac{Dk}{Dt} = \frac{\partial}{\partial x_i}\left[\left(\mu + \frac{\mu_t}{\sigma_k}\right)\frac{\partial k}{\partial x_i}\right] + G_k + G_b - \rho\varepsilon$$

$$\rho\frac{D\varepsilon}{Dt} = \frac{\partial}{\partial x_i}\left(\mu + \frac{\mu_t}{\sigma_\varepsilon}\right)\frac{\partial \varepsilon}{\partial x_i} + C_{1\varepsilon}\frac{\varepsilon}{k}\left(G_k + C_{3\varepsilon}G_b\right) - C_{2\varepsilon}\frac{\varepsilon^2}{k}$$

Where

$$\mu_t = \rho C_\mu \frac{k^2}{\varepsilon}$$

$$\frac{Dk}{Dt} = \frac{\partial k}{\partial t} + \frac{\partial ku}{\partial x_i} \qquad \text{and} \qquad \frac{D\varepsilon}{Dt} = \frac{\partial \varepsilon}{\partial t} + \frac{\partial \varepsilon u}{\partial x_i}$$

10. The DPM predicts the trajectory of particles in a fluid flow by integrating the following force balance with a Lagrangian reference frame. Where F_D, g_x and F_x are drag force, gravity and other force effects acting on the particles, respectively.

$$\frac{du_p}{dt} = F_D\left(u - u_p\right) + g_x \frac{\left(\rho - \rho_p\right)}{\rho_p} + F_x$$

$$F_D = \frac{18\mu}{\rho_p D_p^2} * \frac{C_D \, Re_p}{24}$$

$$Re_p = \frac{\rho D_p \left|u_p - u\right|}{\mu}$$

11. The forces acting on the solid particles with the DPM formulations, through the F_x term include the virtual mass effect, pressure effects and the Saffman lift force, respectively. Where K is a constant and d_{ij}, d_{lk} and d_{kl} are deformation tensors.

$$F_x = \frac{1}{2}\frac{\rho}{\rho_p}\frac{d}{dt}\left(u - u_p\right)$$

$$F_x = \left(\frac{\rho}{\rho_p}\right) u_p \frac{\partial u}{\partial x}$$

$$F_i = \frac{2K\nu^{\frac{1}{2}}\rho d_{ij}}{\rho_p D_p \left(d_{lk} d_{kl}\right)^{\frac{1}{4}}} \left(u_i - u_{i_p}\right)$$

Nomenclature

General Nomenclature

F = external body force (kg m s^{-2})
g = gravitational acceleration (m s^{-2})
p = pressure (N m^{-2})
Re = Reynolds number
u = horizontal velocity or velocity component (m s^{-1})
v = vertical velocity (m s^{-1})
w = z direction velocity (m s^{-1})
t = time (s)
x = horizontal spatial co-ordinate
y = vertical spatial co-ordinate
z = depth spatial co-ordinate

Greek Symbols

μ = phase viscosity (kg m^{-1} s^{-1})
ρ = phase density (kg m^{-3})

Subscripts and Superscripts
i = co-ordinate index
j = co-ordinate index

Algebraic Slip Mixture Model Nomenclature
D = diffusion variable for the drift velocity
d = particle diameter (m)
f = dimensionless friction factor
S = source term
V = slip velocity ($m\ s^{-1}$)

Greek Symbols
α = volume fraction

Subscripts and Superscripts
c = continuous phase
k = phase index
m = mixture variable
n = number of phases
p = phase index
$\rightarrow$ = mass averaged variable

Discrete Particle Model Nomenclature
D = particle diameter (m)
d = deformation tensor
K = constant = 2.594

Greek Symbols
ν = kinematic viscosity (μ/ρ) ($m^{-4}\ s^{-1}$)

Subscripts and Superscripts
D = drag
k = co-ordinate index
l = co-ordinate index
p = particle index
x = co-ordinate depend force effect

k-ε turbulence Nomenclature
$C_{1\varepsilon}$ = constant for the turbulent dissipation of energy = 1.44
$C_{2\varepsilon}$ = constant for the turbulent dissipation of energy = 1.92
$C_{3\varepsilon}$ = constant for the turbulent dissipation of energy
C_{μ} = turbulent viscosity constant = 0.09
G = generation of turbulent energy
k = kinetic energy
Y_M = contribution of fluctuating dilation in compressible turbulence

Greek Symbols
ε = rate of dissipation of turbulent energy
σ_k = turbulent Prandtl number for the kinetic energy = 1
σ_ε = turbulent Prandtl number for the rate of dissipation of energy = 1.3

Subscripts and Superscripts
b = buoyancy
k = kinetic energy
M = Mach number
t = turbulent

References

1. Sanyal, J. Vásquez, S. Roy, S. and Duduković M. P. (1999) Numerical simulation of gas-liquid dynamics in cylindrical bubble column reactors, *Chemical Engineering Science*, **54**, 5071-5083
2. Degaleesan, S. (1997) Fluid dynamic measurements and modelling of liquid mixing in bubble columns, D.Sc. Thesis, Washington University, St. Louis, Missouri, USA.
3. Krishna, R. van Baten, J. M., and Urseanu, M.I. (2000) Three-phase Eulerian simulations of bubble column reactors operating in the churn-turbulent regime: a scale up strategy *Chemical Engineering Science*, **55**, 3275-3286
4. Torvik, R. and Svendsen, H. F. (1990) The modelling of slurry reactors a fundamental approach, *Chemical Engineering Science*, **45**, 2325-2332
5. Ranade, V. V. (1992) Flow in bubble columns: some numerical experiments, *Chemical Engineering Science* **47**, 1857-1869
6. Ranade, V. V. (1997) Numerical simulation of the dynamics of two-phase gas-liquid flows in bubble columns, Chemical Engineering Research and Design Part A: Transactions of the Institute of Chemical Engineers **75**, 14-23
7. Becker, S. Sokolichin, A. and Eigenberger G. (1994) Gas-liquid flow in bubble columns and loop reactors, Part 2, *Chemical Engineering Science* **49**, 5747-5762
8. Sokolichin, A. and Eigenberger G. (1994) Gas-liquid flow in bubble columns and loop reactors, Part 1, *Chemical Engineering Science* **49**, 5735-5746
9. Lapin, A. and Lübbert, A. (1994) Numerical simulation of the dynamics of two-phase gas-liquid flows in bubble columns, *Chemical Engineering Science* **49**, 3661-3674
10. Devanathan, N. Duduković, M. P. Lapin, A. and Lübbert, A. (1995) Chaotic flow in bubble column reactors, *Chemical Engineering Science* **50**, 2661-2667
11. Lapin, A. Lübbert, A. and Paaschen, T. (1996) Fluid dynamics in bubble column bioreactors: experiments and numerical simulations, *Biotechnology and Bioengineering* **52**, 248-258
12. Lapin, A. Lübbert, A. Sokolichin, A. and Eigenberger G. (1997) Dynamical numerical simulation of gas-liquid two-phase flows Euler/Euler versus Euler/Lagrange, *Chemical Engineering Science* **52**, 611-626
13. Sokolichin, A. and Eigenberger, G. (1999) Applicability of the standard k-epsilon turbulence model to the dynamic simulation of bubble columns: Part I. Detailed numerical simulations, *Chemical Engineering Science* **54**, 2273- 2284
14. Delnoij, E. Lammers, F. Kuipers, J. A. M. and van Swaaij, W. P. M. (1997 A) Dynamic simulation of dispersed gas-liquid two-phase flow using a discrete bubble model, *Chemical Engineering Science* **52**, 1429-1458
15. Delnoij, E. Kuipers, J. A. M. and van Swaaij, W. P. M. (1997 B) Computational fluid dynamics applied to gas-liquid contactors, *Chemical Engineering Science* **52**, 3623-3638
16. Delnoij, E. Kuipers, J. A. M. and van Swaaij, W. P. M. (1997 C) Dynamic simulation of gas-liquid two-phase flow: effect of column aspect ratio on the flow structure, *Chemical Engineering Science* **52**, 3759-3772
17. Delnoij, E. Kuipers, J. A. M. and van Swaaij, W. P. M. (1999) A three-dimensional CFD model for gas-liquid bubble columns, *Chemical Engineering Science* **54**, 2217- 2226
18. Chen, J. J. J. Jamialahmadi, M. and Li, S. M. (1989) Effect of liquid depth on the circulation in bubble columns: a visual study, *Chemical Engineering Research and Design* **67**, 203
19. Manninen, M. Taivassalo V. and Kallio, S. (1996) On the mixture model for multiphase flow, *VTT Publications*, **288**, IBSN 951-38-4946-5
20. Fluent 5 User's Guide (1998) Fluent Incorporated, Lebanon, New Hampshire, US (www.fluent.com)
21. Ishii, M. (1975) Thermo-fluid Dynamic Theory of Two-phase Flow, Paris, Eyrolles
22. Ishii, M. and Zuber, N. (1979) Application of general constitutive principles to the derivation of multidimensional two-phase flow equations, *AIChE Journal* **25**, 843-854
23. Drew, D. A. and Lahey, R. T. (1979) Application of general constitutive principles to the derivation of multidimensional two-phase flow equations, *International Journal of Multiphase Flow* **5**, 243-264
24. Drew, D. A. (1983) Mathematical modelling of two-phase flow, *Ann. Rev. of Fluid Mechanics* **15**, 261-291
25. Gidaspow, D. (1994) Multiphase flow and fluidisation: Continuum and kinetic theory descriptions, San Diego, Academic Press.
26. Simonin, O. (1990) Eulerian formulation for particle dispersion in turbulent two-phase flows, Proceedings of the 5th Workshop on Two-Phase Flow Predictions, March 19-22 Erlangen, FRG. Jülich: Kernforschungsanlage Jülich. 156-166
27. Ungarish, M. (1993) Hydrodynamics of suspensions: Fundamentals of centrifugal and gravity separation. Berlin: Springer
28. Verloop, W. C. (1995) The inertial coupling force, *International Journal of Multiphase Flow* **21**, 929-933

29. Launder, B. E. and Spalding D. B. (1974) The numerical computation of turbulent flows, *Computer Methods in Applied Mechanics and Engineering*, **3**, 269-289
30. Pfleger, D. Gomes, S. Gilbert, N. and Wagner H. –G. (1999) Hydrodynamic simulations of laboratory scale bubble columns fundamental studies of the Eulerian-Eulerian modelling approach, *Chemical Engineering Science* **54**, 5091-5099
31. Leonard, B. P. (1979) A stable and accurate convective modelling procedure based on quadratic upstream interpolation, *Computer Methods in Applied Mechanics and Engineering* **19**, 59-98
32. van Doormal, J. P. and Raithby, G. B. (1984) Enhancements of the SIMPLE method for predicting imcompressible fluid flows, *Numerical Heat Transfer*, **7**, 147-163